Jagannath University Journal of Science
Volume 08, Number I, December 2021, pp. 74–80
https://jnu.ac.bd/journal/portal/archives/science.jsp
ISSN 2224-1698

JnUJSci

Photocatalytic and Antibacterial Activity Assessment of Spherical Zinc Oxide Nanoparticles Synthesized by Chemical Precipitation Method

Research Article

Md. Shah Alam, S. M. Abu Nayem, Biswajit Kumar Biswas, Muhammad Zamir Hossain*

Department of Chemistry, Jaganath University, Dhaka 1100, Bangladesh

Received: 07 September 2021
Accepted: 15 December 2021

Abstract: In this paper, we report the synthesis of spherical zinc oxide (ZnO) nanoparticles (NPs) via chemical precipitation method, as well as their photocatalytic and antibacterial activity assessment. ZnO NPs were synthesized using zinc acetate dihydrate [$Zn(CH_3COO)_2.2H_2O$] as a precursor and sodium hydroxide (NaOH) as a reducing agent, and then characterized using various techniques of ultraviolet-visible spectroscopy (UV–vis), X-ray diffraction (XRD), transmission electron microscopy (TEM), selected area diffraction pattern (SAED) and energy dispersive X-ray diffraction (EDX) spectroscopy. The product's characteristic UV–vis peak at 358 nm (λ_{max}) suggested primarily the formation of ZnO NPs. XRD pattern of the product revealed hexagonal wurtzite phase of ZnO. TEM analysis revealed the spherical nature of synthesized ZnO NPs with an average particle size of 90 nm. EDS elemental analysis identified the presence of Zn and O. Under UV light irradiation, the efficiency of photodegradation of methylene blue (MB) dye by synthesized ZnO NPs resulted in 86% with pseudo-first-order reaction kinetics and a rate constant of 0.01159 (min^{-1}). Also, ZnO NPs showed a zone inhibition of 15 mm on the cell wall of *Escherichia Coli (E. coli*) bacterium at a dosage of 70µL at a concetration of 100 mg/L.

Keywords: *Zinc oxide nanoparticles ● Precipitation ● TEM ● Escherichia coli ● Photodegradation ● Methylene blue.*

1. Introduction

Bacterial contamination in food and healthcare services is rapidly growing. In most cases of food poisoning, the food is contaminated by bacteria like *E. coli*. Foodborne diseases can cause disability; these diseases are caused by toxins produced by bacteria or other toxic compounds in food, which can cause severe diarrhea, toxic shock syndrome, severe infections like meningitis, and even death (Hernández-Cortez et al. 2017). Antibacterial active compounds are being sought to address this problem.

On the other hand, different dyes from industrial effluents are persistent due to their complicated chemical structure. Because of the long persistent of such colors in the environment, they end up causing a lot of pollution. MB, for example, is a heterocyclic dye molecule that is employed as a color and a medicinal medication. It can enter the human body through effluents from the textile, paper, and pharmaceutical sectors, and these poisonous, carcinogenic, and persistent dyes are not only harmful to individuals, but also to the environment. Furthermore, the presence of MB in drinking water is harmful to one's health since it causes irritation of the eyes and skin, hemolytic anemia, nausea, vomiting, and abdominal pain. As a result, it's critical to get MB out of the water. Pollution from MB and other dyes is steadily growing, as are problems with the environment. Hence, dye degradation active materials are urgently required because of the issues.

*Corresponding author : Muhammad Zamir Hossain
E-mail : zamir@chem.jnu.ac.bd

Therefore, to solve the above-mentioned two problems a material is needed which meets both the requirements. Interestingly, ZnO NP is such an agent which can be utilized to eliminate food poisoning and dye pollution problems. ZnO, an active *n*-type semiconducting metal oxide, has received considerable attention in the field of nanomaterials. Because, ZnO has unique chemical, physical, and biological features (Mohammadi et al. 2018). As a result, ZnO is a good material for making nanoscale devices, Catalysis and treating pathogens. Additionally, ZnO is abundant in nature and is safe for the environment.

ZnO NPs have been shown to have antibacterial properties against Gram-negative and Gram-positive bacteria (Dadi et al. 2019), (Elumalai et al. 2015). ZnO NPs have been discovered to have significant antibacterial and antimicrobial action because they can easily engage with bacterial surfaces and damage them by structural aberration or toxification. In addition, dye degrading characteristics of ZnO have been demonstrated on several dyes (Prabakaran and Pillay 2019), (Ajmal et al. 2014), (Balcha, Yadav, and Dey 2016). Photodegradation using ZnO NPs is a recent, clean, and cost-effective option for treating dye-polluted water on a wide scale.

Nano ZnO has a greater surface area to volume ratio than micron-sized ZnO, making it superior to micron-sized ZnO for a variety of applications of dye degradation, nanomedicine, and many other areas of nanotechnology (Augustine et al. 2017), (Gebre and Sendeku 2019), (Augustine et al. 2019), (Chavali and Nikolova 2019), (Doolittle et al. 2003). For the above mentioned characteristics, ZnO has been a good choice in recent years for many appliactions (Manjunatha et al. 2019), (López and Rodrguez 2017), (Balram et al. 2019), (Joel et al. 2016), (López and Rodrguez 2017), (Balram et al. 2019), (Joel et al. 2016), (López and (Srinivasan and Manikandan 2017). Also, ZnO granules were found to have antibacterial action against several bacterial strains in a previous study (Judith and Espitia 2012).

It is obvious from the preceding explanation that ZnO may serve as both an antibacterial agent and a photocatalyst due to its unique chemical, physical, and biological capabilities. As a result, developing a simple and cost-effective approach for synthesizing ZnO NPs is important. ZnO NPs may be synthesized by some methods like chemical, hydrothermal, chemical vapor deposition, sol-gel, solvothermal, etc. (Alam and Zamir 2021), (NaveedUlHaq et al. 2017). Chemical precipitation is one of the most advantageous of those approaches since it requires only basic equipment and a cheap solvent of water (Lingaraju et al. 2015), (Dobrucka and Dugaszewska 2015), (Suresh et al. 2018), (Chen et al. 2008).

There are many independent reports on ZnO NPs used as either photocatalyst or antibacterial agents. However, according to our survey, utilizing ZnO NPs for testing antibacterial agents and photocatalysts for dye degradation combining is not found. Therefore, we synthesized ZnO NPs by the chemical precipitation method and characterized them by analytical techniques. The evaluation of ZnO NPs' antibacterial activity against *E. coli* using the disc agar diffusion method and photocatalytic degradation of MB using UV light irradiation is described in this article. Finally, the results are evaluated.

2. Experimental

2.1 Materials

Zinc acetate dihydrate [$Zn(CH_3COO)_2.2H_2O$] and NaOH were purchased from Sigma Aldrich. Both compounds were analytical grade and used without further purification. Bacteria culture media tryptone soya agar and tryptone broth was supplied by Oxion, UK. Muller Hinton agar was provided by Himedia, India. The thickness of the agar was 5 mm. The petri dish measured 90 mm by 15 mm in size. Methylene Blue ($C_{16}H_{18}ClN_3S$), MW 319.85 g/mol, 95 % pure, was supplied by Merck, India. Throughout the experiment, distilled water was used.

2.2 Synthesis of ZnO NPs

In the beginning, a 50 mL aqueous solution of zinc acetate dihydrate [$Zn(CH_3COO)_2.2H_2O$] was prepared. After that, an aqueous solution of sodium hydroxide (NaOH) was progressively dropped into the aforesaid solution while vigorously swirling. $Zn(CH_3COO)_2.2H_2O$ and NaOH had a molar ratio of 1 : 2. After 6 hours of stirring at room temperature, the fluid turned milky, indicating particle production. The product was collected and centrifuged for 20 minutes at 10100 rpm three times before being rinsed with double distilled water. The product was dried at 100 °C for 3 hours and calcined at 550 °C for 6 hours before characterization.

2.3 Characterization of synthesized ZnO NPs

Primary characterization of the ZnO NPs production was performed through UV–vis at room temperature using a spectrophotometer, UV-1800, Shimadzu, Japan, with a wavelength between 200 nm and 800 nm and quartz cuvettes with a path length of 10 mm. An X-ray diffractometer (Phillips X'Pert PRO PW 3040, Netherlands) using CuK radiation in a 2θ-θ configuration was used to analyze the crystal structure of the produced products. At a scanning rate of 0.02°/0.6 s, the scanned value of 2 angles was between 10° and 70°. Data from the Joint Committee for Powder Diffraction Studies (JCPDS) file for silver were compared to the measured data (BD Card No. 01-070-8072). The particle size and shape of the produced ZnO NPs were examined using

transmission electron microscopy (TEM, TALOS F200X, 200 KeV, Netherlands) with 200 kV acceleration voltages. The calcined product was re-dispersed in water, and the ZnO NPs dispersion droplets on the TEM grid were used to prepare the TEM grid. Using an energy dispersive X-ray spectrometer part of the same instrument, EDX was used to determine the existence of elements and their percentage.

2.4 Antibacterial assay

The bacterial strain (*E. coli*) was subcultured on tryptone soya agar (TSA) media. One loopful colony was selected from a freshly cultured plate and used to inoculate 9 mL of tryptone soya broth (TSB) into a 37 ^{0}C incubator overnight to match the turbidity of the 0.5 McFarland standard (Cell density = 1.5 108 CFU/mL).

2.5 Photodegradation of methylene blue (MB) under UV light irradiation

The photodegradation of MB under UV light irradiation was used to assess the photocatalytic activity of ZnO NPs. In 100 mL of an aqueous solution containing 10 ppm MB, 50 mg of photocatoyst (ZnO NPs) was added. A colloidal solution was created before irradiation by magnetic stirring the suspension solution for 1 hour to achieve adsorption-desorption equilibrium. The photocatalytic experiment was conducted at room temperature using a beaker with a magnetic stirrer and three UV tubes. To prevent light from entering the reaction media, the entire setup was wrapped in a box with aluminum foil. The solution in the beaker was subjected to UV radiation at normal temperature and stirring settings. In a beaker with a stirring, the MB solution with ZnO noanocatalyst was placed. First, the process was run for 60 minutes under dark adsorption to assure adsorption/desorption equilibrium. Then, the solution was then irradiated for 3.5 hours at 30-minute intervals, then centrifuged for 10 minutes at 4000 rpm to separate photocatalyst particles for analysis. A double beam UV-visible spectrophotometer was used to examine the deterioration of the resultant solutions (SHIMAZU 1800). After that, using equation (1), the proportion of photocatalytic degradation was computed (Balcha, Yadav, and Dey 2016).

Percentage of photocatalytic degradation = $\frac{A_0 - A_t}{A_0} \times 100\% \ldots . (1)$

where A_0 denoted the initial dye absorbance and A_t in the presence of ZnO at time *t*.

3. Results and discussion

3.1 UV–vis spectroscopy

UV–vis spectroscopic measurement revealed the formation of ZnO NPs as the primary evidence. UV–vis spectroscopy is a method for determining the structural characterization of NPs. Figure 1 depicts the UV–vis spectrum of synthesized ZnO NPs. At 358 nm, a sharp intense absorption peak was seen, which was identical to the ZnO NPs absorption band as described in the literature (Lingaraju et al. 2015).

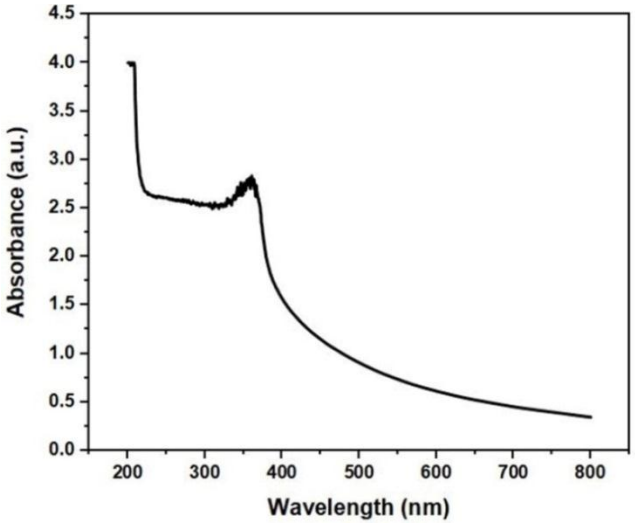

Figure 1. UV–vis spectrum of synthesized ZnONPs.

3.2 X-ray diffraction (XRD) analysis

The crystalline nature and phase structure of produced ZnO NPs were validated by XRD analysis. Figure 2 depicts the XRD pattern of prepared ZnO NPs. When compared to standard card [No. JCPDS 89-1397], the matching diffractogram in 2θ range 20–70^0 with a Braggs reflection of (100), (002), (101), (102), (110), (103), and (112) at 31.75^0, 34.40^0, 36.26^0, 47.53^0, 56.61^0, 62.90^0, and 69.06^0, respectively revealed hexagonal wurtzite phase. Furthermore, there was no identified signal due to impurity, indicating that a single-phase structure of ZnO NPs had developed (Tshabalala, Dejene, and Swart 2012), (Suresh, Pradheesh, and Alexramani 2018).

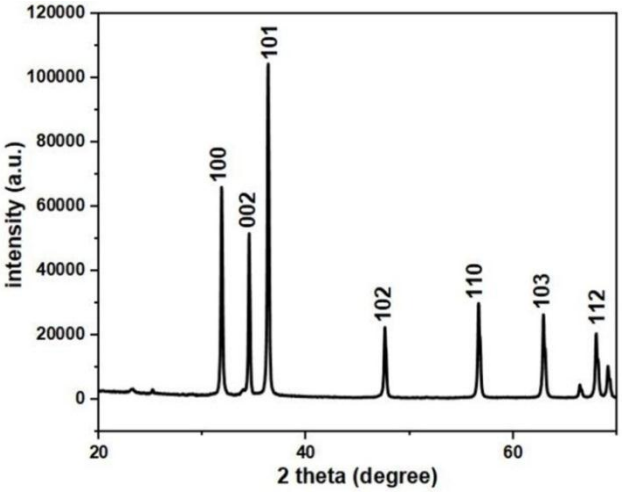

Figure 2. XRD pattern of synthesized ZnO NPs.

3.3 TEM, SAED, and EDX analysis

The surface morphology of synthesized NPs was characterized using TEM analysis. Figure 3(a) shows a typical TEM image of synthesized ZnO NPs which indicated spherical shape particles were synthesized. To know the average particles size, the diameters of about 100 NPs were measured and calculated the average value. The average size (diameter) of the ZnO NPs to be found 90 nm. Figure 3 (b) shows the SAED of ZnO NPs. Crystallized particles were exhibited from it. The diffraction rings on the SAED image matched with the peaks in the XRD pattern, this result also proved the hexagonal wurtzite structure of ZnO NPs.

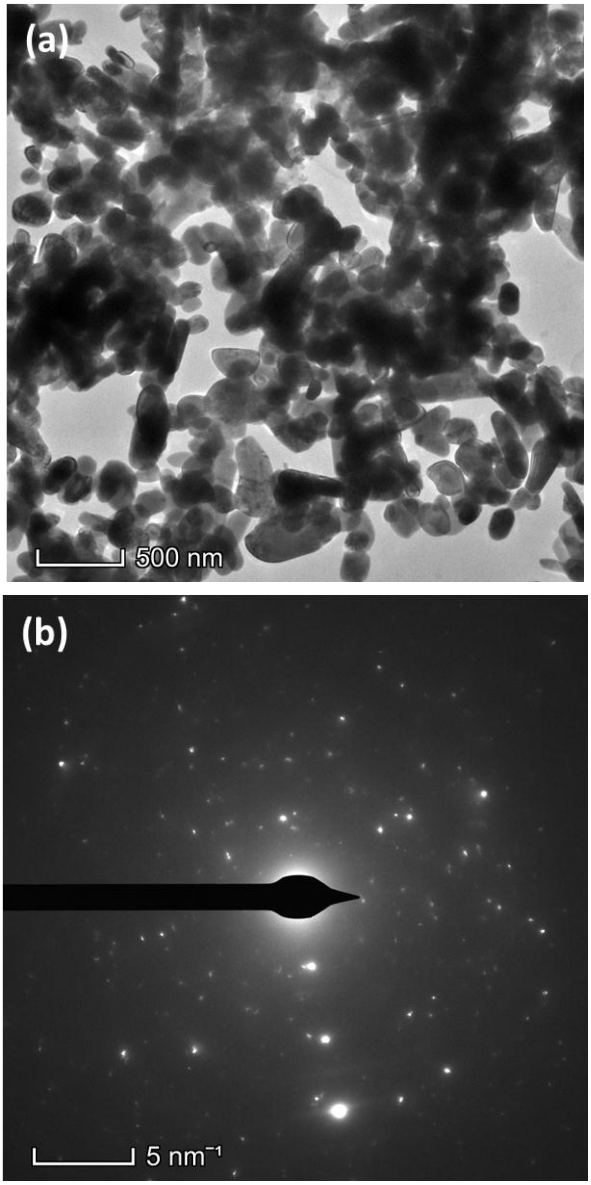

Figure 3. (a) TEM images and (b) SAED images of synthesized ZnO NPs.

Figure 4 shows the results of an elemental composition investigation of produced ZnO NPs using EDX spectroscopy (Kathiwada et al. 2018), (Nagajyothi et al. 2013), (Kathiwada et al. 2018), (Kathiwada et al. 2018), (Kathiwada et al. 2018), (Kathiwada et al. 2018), (Kathiwada et al. 2018), (Kathiwada (Taylor et al. 2015). This EDS data validated the synthesis of ZnO NPs by adding another strong sharp peak to the spectrogram due to oxygen. Two very minor peaks are shown, which could be related to the copper grid used to capture the sample. The.ratio of atom of Zn and O is found 1 : 1.

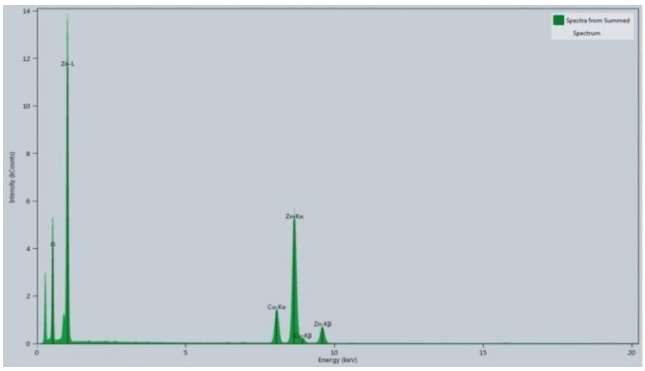

Figure 4. EDX spectrum of synthesized ZnO NPs.

3.4 Antibacterial activity of synthesized ZnO NPs

The antibacterial activity of produced NPs was tested against *E. coli* bacteria using the disc agar diffusion method after an 18-hour incubation period. ZnO NPs were found to have a strong inhibitory impact on *E. coli* bacteria. The actual mechanism of antibacterial action is uncertain. However, according to the literature review, surface reactive oxygen is formed on the surface of ZnO NPs, which causes pathogens to dyes (Shah, Boruah, and Parween 2015), (Pal et al. 2018). Figure 5 shows the zone of inhibition, which was measured at 15 mm at a dose of 10μg L^{-1}. The results were compared to the common antibiotic amoxicillin.

Figure 5. *E. coli* bacterial zone inhibition by the synthesized ZnO NPs at a concentration of 70μg mL.

3.5 Photodegradation of MB under UV light irradiation

The absorption against the wavelength of 10 ppm MB dispersion by the ZnO NPs photocatalyst is shown in Figure 6. The bulb was then turned up to speed up the photocatalytic process. After the dark treatment, the time was kept track of. As a control, the MB solution was leveled without the catalyst. After 150 minutes of UV lamp exposure, the MB solution with catalyst transformed into decolorization, suggesting that MB was degraded under these conditions.

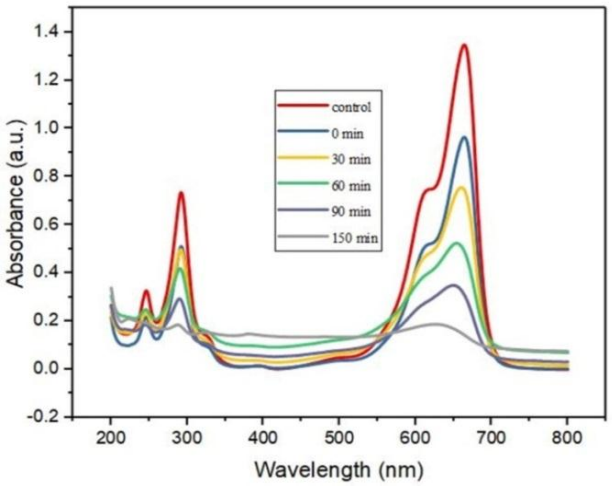

Figure 6. UV–vis spectrum of MB photodegradation by ZnO NPs photocatalyst.

Based on equation (1), the efficiency was found to be 85.93 percent at time 150 minutes, as illustrated in Figure 7. Literature data of efficiency (86%) is comparable with the data obtained in this study (Isai and Shrivastava 2019). Probably, by controlling the size of the ZnO NPs, more efficiency would be possible since the smaller particles provide Larger surface areas and hence the higher photocatalytic activity.

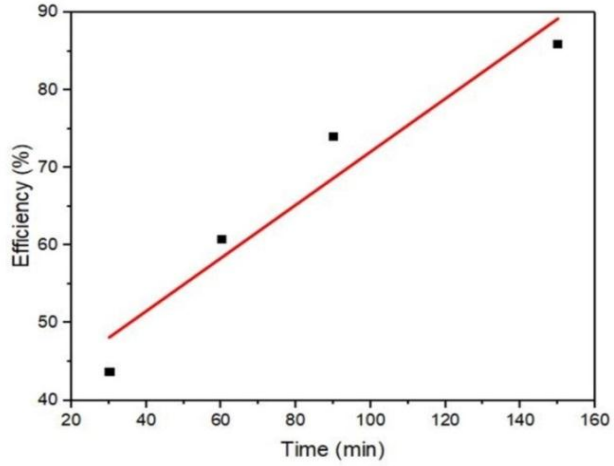

Figure 7. Efficiency calculation of MB photodegradation under UV irradiation by ZnO NPs.

The kinetics of dye degradation were determined using the formula ln (A_0/A_t) versus time. The dye absorbance after self– photolysis and at different irradiation periods are represented by A_0/A_t respectively. The linear fit of ln (A_t/A_0) vs time suggested a pseudo-first-order kinetics pattern of MB photodegradation (Figure 8). The rate constant was determined to be 0.01159 (min^{-1}) (Raj et al., 2020) (Chen et al. 2017).

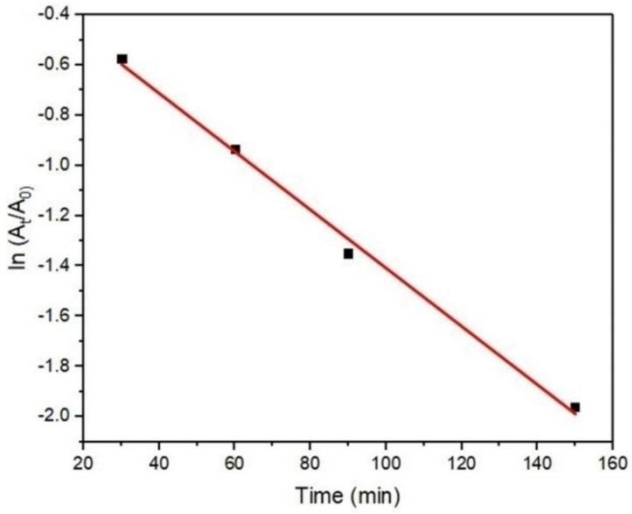

Figure 8. Kinetics study of MB photodegradation under UV irradiation.

Conclusions

We successfully synthesized spherical ZnO NPs by the chemical precipitation method in this investigation. UV–vis spectroscopy, TEM, XRD, SAED, and EDS suggest the formation of spherical ZnO NPs with an average diameter of 90 nm. With an efficiency of 86 %, prepared ZnO NPs showed good photocatalytic activity in the photodegradation of MB solution. Higher efficiency may be obtained by controlling the particle size. The rate constant was found to be 0.01159 (min^{-1}) in the kinetic analysis. At a dosage of 100 10µg mL, the antibacterial activity of ZnO NPs against *E. coli* showed a good response, with a zone of inhibition of 15 mm.

Acknowledgments

This research was supported by a Jagannath University Research Grant 2018. We acknowledge the analytical support of the Atomic Energy Centre, Dhaka.

Declarations of interest: none

References

Alam MS, Hossain MZ**.** (2021). A Simple Hydrothermal Protocol for the Synthesis of Zinc Oxide Nanorods, *Jagannath Univ. J. Sci.*, 7(2): 75–80**.**

Ajmal A, Majeed I, Riffat N, Idriss H Nadeem MA. (2014). Principles and Mechanisms of Photocatalytic Dye Degradation on T_1O_2 Based Photocatalysts: A Comparative Overview. *RSC Adv.*, 4(70): 37003–26.

Augustine R, Mathew PA, Alejandro S. (2017). Metal Oxide Nanoparticles as Versatile Therapeutic Agents Modulating Cell Signaling Pathways: Linking Nanotechnology with Molecular Medicine. *Appl.Mater. Today*, 7: 91–103.

Balcha A, Yadav OP, Dey T. (2016). Photocatalytic Degradation of Methylene Blue Dye by Zinc Oxide Nanoparticles Obtained from Precipitation and Sol-Gel Methods. *Environ. Sci. Pollut. Res. Int.*, 23(24): 25485–25493.

Bhuyan B, Paul B, Dhar D, Sankar S. (2016). Facile Synthesis and Characterization of Zinc Oxide Nanoparticles and Studies of Their Catalytic Activity towards Ultrasound-Assisted Degradation of Metronidazole. *Mater. Lett.*, 168: 158–62.

Bomila R, Srinivasan S,Gunasekaran S and Manikandan A. (2017). Enhanced Photocatalytic Degradation of Methylene Blue Dye, Opto-Magnetic and Antibacterial Behaviour of Pure and La-Doped ZnO Nanoparticles. *J Supercond Nov Magn*, 31:855–864.

Chavali MS, Nikolova MP. (2019). *Metal Oxide Nanoparticles and Their Applications in Nanotechnology*. *SN Applied Sciences, 1: 607*.

Chen C, Liu P, Lu C. (2008). Synthesis and Characterization of Nano-Sized ZnO Powders by Direct Precipitation Method. *Chem. Eng. J.*, 144(3): 509–13.

Chen X, Wu Z, Liu D, Gao Z. (2017). Preparation of ZnO Photocatalyst for the Efficient and Rapid Photocatalytic Degradation of Azo Dyes. *Nanoscale Res. Lett.*, 12: 143.

Dadi R, Azouani R, Traore M, Mielcarek C, Kanaev A. (2019). Antibacterial Activity of ZnO and CuO Nanoparticles against Gram Positive and Gram Negative Strains. *Mater. Sci. Eng. C*, 104: 109968.

Deepak B, Lian K, Sebastian N. (2019). Ultrasonics - Sonochemistry Ecofriendly Synthesized Reduced Graphene Oxide Embellished Marsh Marigold-like Zinc Oxide Nanocomposite Based on Ultrasonication Technique for the Sensitive Detection of Environmental Pollutant Hydroquinone. *Ultrasonics - Sonochemistry* 58: 104650.

Dobrucka R and Długaszewska J. (2015). Biosynthesis and Antibacterial Activity of ZnO Nanoparticles Using Trifolium Pratense Flower Extract. *Saudi J. Biol. Sci*, 23: 517–523.

Doolittle WA, Namkoong G, Carver AG, and Brown AS. (2003). Challenges and Potential Payoff for Crystalline Oxides in Wide Bandgap Semiconductor Technology. *Solid-State Electro*n. 47: 2143–47.

Elangovan SV, Chandramohan V, Sivakumar N, Senthil TS, (2015). Synthesis and Characterization of ZnO Nanoparticles at Different Molarity Concentrations for Photocatalytic Applications. *Desalin. Water Treat.* 57: 9671-9678.

El-Nour KMMA, Eftaiha A, Al-Warthan A, Reda AA, Ammar. (2010). Synthesis and Applications of Silver Nanoparticles. *Arabian J. Chem.*, 3(3): 135–40.

Elumalai K, Velmurugan S, Ravi S,Kathiravan V, Ashokkumar S, (2015). Materials Science in Semiconductor Processing Bio-Fabrication of Zinc Oxide Nanoparticles Using Leaf Extract of Curry Leaf (Murraya Koenigii) and Its Antimicrobial Activities. *Mater Sci Semicond Process.* 34: 365–72.

Espitia PJP, Soares NFF, Coimbra JSR, Andrade NJ, Cruz RS, Medeiros EAA, (2012). Zinc Oxide Nanoparticles : Synthesis , Antimicrobial Activity and Food Packaging Applications. *Food Bioprocess Technol.* 5 : 1447–64.

Gebre S H, andSendeku MG. (2019). New Frontiers in the Biosynthesis of Metal Oxide Nanoparticles and Their Environmental Applications: An Overview. *SN Appl. Sci. 1: 928*.

Hernández-Cortez, Cecilia et al. 2017. Food Poisoning Caused by Bacteria (Food Toxins). *Poisoning - From Specific Toxic Agents to Novel Rapid and Simplified Techniques for Analysis*.

Isai, K.A., Shrivastava, V.S. (2019). Photocatalytic degradation of methylene blue using ZnO and 2%Fe–ZnO semiconductor nanomaterials synthesized by sol–gel method: a comparative study. *SN Appl. Sci.* 1: 1247.

Joel C, Badhusha MSM and John S. (2016). Green Synthesis of ZnO Nanoparticles Using Phyllanthus Embilica Stem Extract and Their Antibacterial Activity. *Der Pharm. Lett.* 8 (11): 218–223.

Kathiwada CP, Kaviyarasu K, Raman G and Swaminathan M. (2018). The Present Work Reports the Green Synthesis of Zinc Oxide Nanoparticles (ZnO NPs). *Journal of Photochemistry & Photobiology, B: Biology*.

Lingaraju K, Naika HR, Manjunath K, Basavaraj RB, Nagabhushana H, Nagaraju G, Suresh D. (2015). Biogenic Synthesis of Zinc Oxide Nanoparticles Using Ruta Graveolens (L.) and Their Antibacterial and Antioxidant Activities. *Appl Nanosci, 6:703–710.*

López Cand Rodríguez-Paez JE. (2017). Synthesis and Characterization of ZnO Nanoparticles : Effect of Solvent and Antifungal Capacity of NPs Obtained in Ethylene Glycol. *Applied Physics A* 123(12): 748.

Manjunatha RL, Usharani KV and Naik D. (2019). Synthesis and Characterization of ZnO Nanoparticles : A Review. *J. pharmacogn. phytochem*, 8(3): 1095–1101.

MohammadiE, Aliofkhazraei M,Hasanpoor M and Chipara M. (2018). Hierarchical and Complex ZnO Nanostructures by Microwave-Assisted Synthesis: Morphologies, Growth Mechanism and Classification. *Crit. Rev. Solid State Mater. Sci*. 43: 415–541.

Nagajyothi P C, Minhan TN, Sreekanth TVM, Lee J, Lee DJ, Lee KD. (2013). Green Route Biosynthesis : Characterization and Catalytic Activity of ZnO Nanoparticles. *Materials Letters*, 108: 160–63.

Naveed Ul HaqA, Nadhman A, Ullah I, Mustafa G, Yasinzai M, Khan I. (2017). Synthesis Approaches of Zinc Oxide Nanoparticles: The Dilemma of Ecotoxicity. *Journal of Nanomaterials*, (2017) Article ID 8510342.

Pal S, Mondal S, Maity J and Mukherjee R. (2018). Synthesis and Characterization of ZnO Nanoparticles Using Moringa Oleifera Leaf Extract : Investigation of Photocatalytic and Antibacterial Activity. *Int. J. Nanosci. Nanotechnol*, 14(2): 111–19.

Prabakaran E and Pillay E. (2019). Synthesis of N-Doped ZnO Nanoparticles with Cabbage Morphology as a Catalyst for the e Ffi Cient Photocatalytic Degradation of Methylene Blue under UV and Visible Light. *RSC Advances*, 9 : 7509–35.

Raj S, Singh H, Trivedi R and Soni V. (2020). Biogenic Synthesis of AgNPs Employing Terminalia Arjuna Leaf Extract and Its Efficacy towards Catalytic Degradation of Organic Dyes. *Scientific reports* 10(1): 9616.

Shah RK, Boruah F and Parween N. (2015). Synthesis and Characterization of ZnO Nanoparticles Using Leaf Extract of Camellia Sinesis and Evaluation of Their Antimicrobial Efficacy. *Int.J.Curr. Microbiol.App.Sci*. 4(8): 444-450.

Shim YJ, Soshnikova V, Amandapadmanaban G, Zuly R, Jimnez E, Markus PJ, Kim YJ, Castro-Aceituno V, Yang DC. (2019). Zinc oxide nanoparticles synthesized by *Suaeda japonica* Makino and their photocatalytic degradation of methylene blue, *Optik*, 182: 1015-1020.

Suresh J, Pradheesh G, Alexramani V, Sundrarajan M, Hong SI. (2018). Green Synthesis and Characterization of Zinc Oxide Nanoparticle Using Insulin Plant (Costus Pictus D . Don) and Investigation of Its Antimicrobial as Well as Anticancer Activities. *Adv. Nat. Sci.: Nanosci. Nanotechnol.9*: 015008.

Tshabalala M A, Dejene BF and Swart HC. (2012). Synthesis and Characterization of ZnO Nanoparticles Using Polyethylene Glycol (PEG). *Physica B: Physics of Condensed Matter*, 407(10): 1668–71.